Band structure in ^{147,149,151}Eu observed via (HI, xn) reactions

J. G. Fleissner, E. G. Funk, F. P. Venezia, and J. W. Mihelich
*University of Notre Dame, Notre Dame, Indiana 46556**
(Received 7 March 1977)

γ rays from levels in ^{147,149,151}Eu have been studied using primarily (^{6,7}Li, $xn\gamma$) reactions. Prompt and delayed γ-γ coincidences, excitation functions, and angular distributions were used to study the in-beam γ rays. Bands with $\Delta I = 2$ built on an $11/2^-$ isomeric state have been observed in all three nuclei and since the energy spacings strongly resemble those of the core nuclei they are interpreted as decoupled bands. The maximum spin observed in the decoupled band is $27/2^-$ for ^{151}Eu and $23/2^-$ for ^{149,147}Eu. Possible unfavored states associated with the $\pi h_{11/2}$ system have also been identified. High spin positive parity states have been observed for ^{147}Eu and ^{149}Eu. The maximum spin observed for each nucleus is $(33/2^+)$ at 4178.1 keV for ^{147}Eu, $(29/2^+)$ at 3042.0 keV for ^{149}Eu, and $(27/2^-)$ at 2118.9 keV for ^{151}Eu. The experimental results for the negative parity bands of ^{149,151}Eu have been compared with predictions of the triaxial rotor plus particle model incorporating a variable moment of inertia. The results of the model calculations give some indication of triaxial shapes for ^{149}Eu and ^{151}Eu although the predictions for the symmetric case are not significantly different from those of the asymmetric case.

[NUCLEAR REACTIONS ^{143,145}Nd(^{7}Li, $3n\gamma$), ^{146,148}Nd(^{6}Li, $3n\gamma$), E=26.0–34.0 MeV; ^{139}La(^{12}C, $4n\gamma$), E=60, 63 MeV; measured $\sigma(E, E_\gamma, \theta)$, γ-γ coin, γ-γ delay. ^{147,149,151}Eu deduced levels, J, π. Enriched targets. Ge(Li) detectors. Triaxial rotor-plus-particle calculations including VMI.]

I. INTRODUCTION

Recently it has been shown using (HI, xn) reactions that many odd-A nuclei in the so-called transitional region between closed shells and strongly deformed nuclei exhibit decoupled band structure. The behavior of these bands has been explained by the rotation-alignment coupling model of Stephens[1] where the odd particle, of angular momentum j, is decoupled from the core and aligned along the rotation axis of the nucleus. The odd particle does not follow the rotation of the core and the nucleus exhibits a band structure with the spin sequence $j, j+2, j+4, \ldots$, and energy spacing similar to the ground-state band of the adjacent even-even nuclei. The positions of the "unfavored" (or partially aligned) states based on the same j shell, however, are very sensitive to various parameters of the nucleus. Although these states are usually weakly populated in (HI, xn) reactions, they provide a critical test for the model used to describe them.

Meyer-ter-Vehn[2] has extended the rotation-alignment model by including γ deformation. This model has had considerable success in explaining whole families of unique-parity states in the A = 190–200 region. Toki and Faessler[3] have further extended the model by using an asymmetric rotor with a variable moment of inertia. This model gives better quantitative agreement for high-spin states than the Meyer-ter-Vehn model and has been applied successfully in the $A \cong 130$ and $A \cong 190$ regions.

In-beam γ-ray investigations have been carried out on many odd-N nuclei in the A = 140–155 transitional region. The odd-A europium nuclei (Z = 63) with A = 147 to 151 have N = 84 to 88, spanning the region from just above the closed shell at N = 82 to just below the onset of the strongly deformed nuclei at N = 90. In this "transition" region the core deformation changes rapidly as a function of neutron number. Evidence for the coexistence of spherical and deformed states in ^{151}Eu has been found by Taketani, Sharma, and Hintz[4] and Burke, Løvhøiden, and Waddington.[5] It would be of interest to see whether or not bands are built on these states and whether similar states exist in the other europium nuclei. Previously, bands built on $\frac{11}{2}^-$ intrinsic states have been observed for some odd neutron nuclei with N = 55 to 89 and for odd proton nuclei with Z = 53 to 59. Several of these nuclei also exhibit bands built on intrinsic levels other than the $\frac{11}{2}^-$ level.

The odd mass Eu nuclei have been studied previously mainly by radioactive decay[6-8] yielding information on states with spin $I \leq \frac{11}{2}$. Some data on other low-spin states have been obtained from Coulomb excitation,[7,8] (d, d'),[9] (p, t) reactions,[4] and proton transfer reactions.[10] All of the odd-A Eu nuclei having A between 143 and 151 possess $\frac{5}{2}^+$ ground states, $\frac{7}{2}^+$ first excited states, and low lying $\frac{11}{2}^-$ isomeric states. In this paper we

present and discuss our in-beam γ-ray spectroscopy results for ^{147,149,151}Eu obtained by (HI, $xn\gamma$) reactions. Theoretical predictions using the rotation-alignment model and asymmetric rotor model will also be presented.

II. EXPERIMENTAL PROCEDURE

The nuclei ^{147,149,151}Eu were studied using (^{6,7}Li, $xn\gamma$) and (^{12}C, $xn\gamma$) reactions with beams produced in the Notre Dame FN tandem accelerator. Self-supporting metallic targets of monoisotopic La and isotopically enriched Nd, rolled to a thickness of 1–5 mg/cm^2, were used. The in-beam γ-ray experiments included excitation function measurements, γ-γ coincidence measurements, and γ-ray angular distributions. The excitation function results were used to assign the more intense γ rays to a particular reaction and to determine the optimum beam energy for the coincidence and angular distribution experiments. A typical excitation function is shown in Fig. 1. The angular distribution measurements were taken with either a 45 or a 60 cm^3 Ge(Li) detector at six or seven angles including 0° and 90°. Normalization of the data was accomplished through the use of an additional Ge(Li) detector fixed at 90°, and correction for dead time was accomplished by a pulser inserted into the test input of the detector preamplifiers.

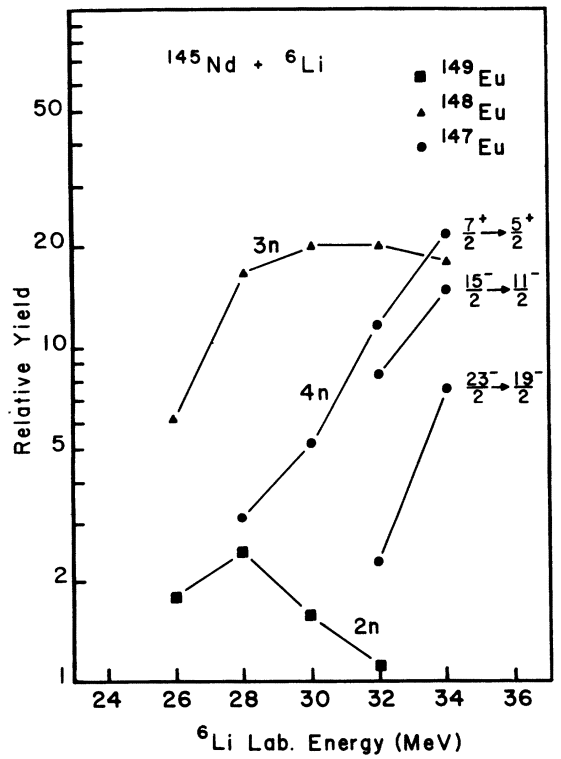

FIG. 1. Relative γ-ray yields as a function of incident projectile energy for the reaction ^{145}Nd(^{6}Li, xn) where $x = 2, 3, 4$. Yields for selected transitions are shown for the $4n$ reaction.

For the coincidence measurements the 45 cm^3 Ge(Li) detector was positioned at 90° and the 60 cm^3 Ge(Li) at the forward angle of 55°. Constant fraction timing was employed with typical resolving times of approximately 80 nsec for an energy range of 0.1 to 2.0 MeV. Three parameter data ($E_{\gamma_1}, E_{\gamma_2}, t_{12}$) were stored on magnetic tape in the event-by-event mode. The three nuclei studied all have low lying $\frac{11}{2}^-$ isomeric states ranging in half-life from 710 nsec for ^{147}Eu to 60 μsec for ^{151}Eu (Ref. 6), and both prompt and delayed coincidence data were obtained. A typical singles spectrum together with prompt and delayed coincidence gated spectra are shown in Fig. 2.

The angular distribution data were analyzed using computer codes and the transition intensities were fitted to the formula $W(\theta) = \alpha_0 + \alpha_2 P_2 + \alpha_4 P_4$ using a weighted least squares program from which the coefficients $A_{22} = \alpha_2/\alpha_0$ and $A_{44} = \alpha_4/\alpha_0$ were then determined. The computer code PARADI was used to obtain mixing ratios and values of σ/J by varying these quantities along with A_{00} and minimizing χ^2. Figure 3 shows a typical plot of χ^2 vs arctanδ for different initial spins. Results for A_{22}, A_{44}, σ/J, and δ are given in Tables I–III. For $|\Delta I| = 1$ transitions an $M1/E2$ admixture is assigned if δ_{12}, the mixing ratio, is considerably different from zero while an $E1$ assignment is made if $\delta_{12} \approx 0$.

III. EXPERIMENTAL RESULTS

A. ^{151}Eu

Angular distribution and coincidence measurements were obtained using the ^{148}Nd(^{6}Li, $3n$) reaction at 32 MeV where it has the largest yield. The information obtained from these measurements for ^{151}Eu is summarized in Table I and consists of γ-ray energies, γ-ray transition intensities, angular distribution coefficients, and σ/J values. The level scheme deduced from this information is shown in Fig. 4.

The 306.1 keV transition was established as preceding the 63 μsec $\frac{11}{2}^-$ state at 197 keV by a delayed coincidence experiment in which the detection of a pulse corresponding to a 306.1 keV event in the "start" counter opened two time gates $\approx$60 μsec apart for a second ("stop") counter which accepted pulses corresponding to the 175 keV transition which depopulates the isomeric level. The half-life value for the $\frac{11}{2}^-$ state which was obtained is consistent with the currently accepted value of

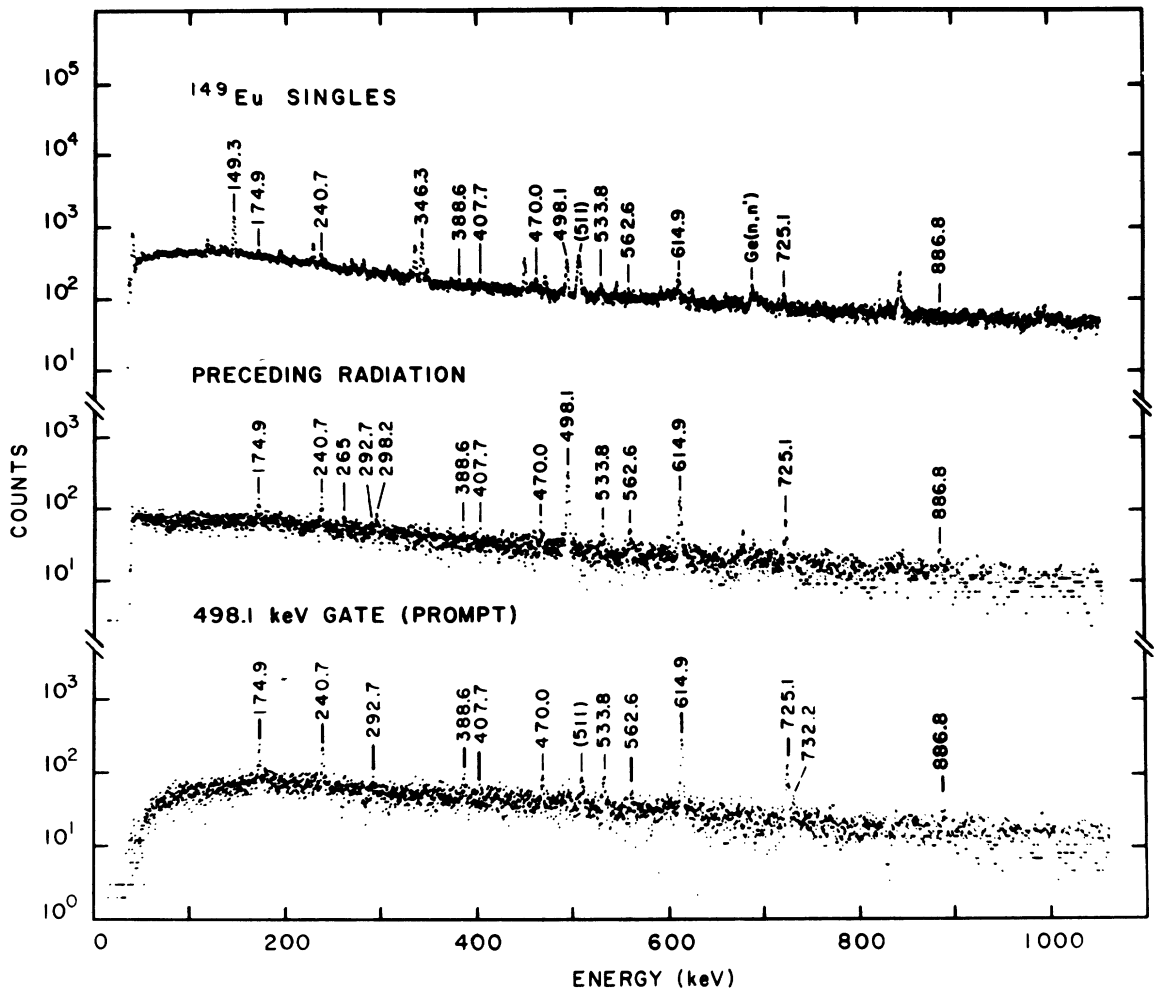

FIG. 2. γ-ray singles, preceding radiation, and prompt coincidence spectra for the ^{146}Nd(^{6}Li, $3n$)^{149}Eu reaction. These spectra are typical of spectra obtained with the reactions producing ^{147}Eu and ^{151}Eu.

63 μsec. The 306.1, 455.2, 546.0, and 615.0 keV transitions were observed to be in prompt coincidence and thus an $\frac{11}{2}^-$ decoupled band up to spin $\frac{23}{2}^-$ and possibly to spin $\frac{27}{2}^-$ is proposed.

The 615.0 keV transition from the $(\frac{27}{2}^-)$ to $\frac{23}{2}^-$ state was weak, but the distribution coefficients obtained, although having large errors, are not inconsistent with an $E2$ assignment for this transition. Also, the similarity in energy between the 615.0 keV transition and the 8^+ to 6^+ transition of the adjacent even-even Sm core (see Fig. 5) is some support for its assignment as a member of the decoupled band.

Two other transitions are observed in the coincidence measurements and these establish a 523.2-429.5 keV cascade feeding the $\frac{15}{2}^-$ level at 503 keV. However, the levels depopulated by these transitions are populated so weakly in this reaction

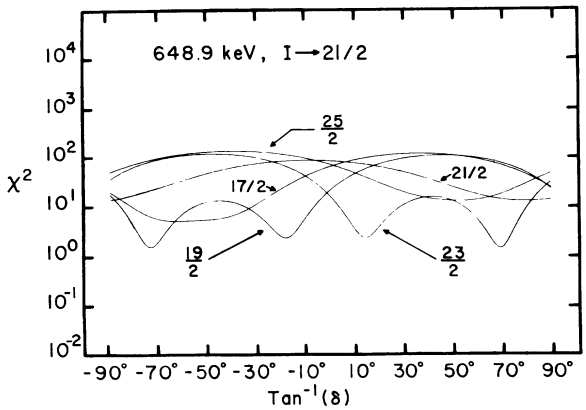

FIG. 3. Typical χ^2 versus $\tan^{-1}\delta$ plot showing angular distribution data for the $I \rightarrow \frac{21}{2}$ (648.9 keV) transition in ^{147}Eu. Plots for different possible initial spins are superimposed.

TABLE I. Transition energies, intensities, and experimental angular distribution results for ^{151}Eu.

E_γ [a] (keV)	Initial level (keV)	I_γ	A_{22}	A_{44}	σ/J	δ	Assignment
306.1	502.7	100.0(10)	0.256(25)	−0.069(28)	0.36(3)	0.035(17)	$E2$, $\frac{15}{2}^- \rightarrow \frac{11}{2}^-$
429.5	932.2	16.0(5)	0.221(75)	−0.014(85)	0.54(85)	0.52(12)	$M1/E2$, $\frac{13}{2}^- \rightarrow \frac{15}{2}^-$
					0.66(13)	0.69(31)	$M1/E2$, $\frac{17}{2}^- \rightarrow \frac{15}{2}^-$
523.2	1455.4	13.8(6)	0.303(90)	0.016(101)			$E2$, $\frac{17}{2}^- \rightarrow \frac{13}{2}^-$ or $E2$, $\frac{21}{2}^- \rightarrow \frac{17}{2}^-$
455.2	957.9	52.5(9)	0.289(38)	−0.117(44)	0.27(6)	0.044(26)	$E2$, $\frac{19}{2}^- \rightarrow \frac{15}{2}^-$
546.0	1503.9	32.6(7)	0.304(51)	−0.112(59)	0.26(18)	0.018(106)	$E2$, $\frac{23}{2}^- \rightarrow \frac{19}{2}^-$
615.0	2118.9	11.5(7)	0.145(140)	−0.086(160)			$E2$, $\frac{27}{2}^- \rightarrow \frac{23}{2}^-$

[a] Uncertainties in the energy are ±0.3 keV.

TABLE II. Transition energies, intensities, and experimental angular distribution results for ^{149}Eu.

E_γ [a] (keV)	Initial level (keV)	I_γ	A_{22}	A_{44}	σ/J	δ	Assignment
174.9	2749.3	11.4(2)	−0.310(29)	0.014(31)	0.21(12)	0.035(35)	$E1$, $\frac{27}{2}^- \rightarrow \frac{25}{2}^+$
240.7	2574.4	23.3(2)	−0.185(22)	0.014(24)	0.23(14)	0.052(26)	$E1$, $\frac{25}{2}^+ \rightarrow \frac{23}{2}^-$
292.7	3042.0	5.3(1)	−0.351(26)	−0.009(58)	$0.28^{+0.15}_{-0.20}$	0.087(70)	$E1$, $\frac{29}{2}^+ \rightarrow \frac{27}{2}^-$
298.2	793.8	<1 [b]					
388.6	1997.5	3.8(1)	0.423(85)	−0.075(93)	$0.44^{+0.23}_{-0.14}$	$-0.70^{+0.35}_{-2.91}$	$M1/E2$, $\frac{21}{2}^- \rightarrow \frac{19}{2}^-$
					$0.37^{+0.19}_{-0.12}$	$+0.65^{+2.70}_{-0.32}$	$M1/E2$, $\frac{17}{2}^- \rightarrow \frac{19}{2}^-$
407.7	2982.1	<11 [c]					
470.0	1997.5	8.5(2)	0.208(55)	−0.016(58)	0.48(22)	$-0.02^{+0.18}_{-0.21}$	$E2$, $\frac{21}{2}^- \rightarrow \frac{17}{2}^-$ or $E2$, $\frac{17}{2}^- \rightarrow \frac{13}{2}^-$
498.1	933.7	100.0(15)	0.321(32)	−0.095(36)	0.30(20)	0.009(11)	$E2$, $\frac{15}{2}^- \rightarrow \frac{11}{2}^-$
516.2	665.5	7.7(3)	0.412(39)	0.194(100)	$0.35^{+0.15}_{-0.05}$	$-3.1^{+1.3}_{-2.5}$	$M1/E2$, $\frac{9}{2}^+ \rightarrow \frac{7}{2}^+$
533.8	1527.5	18.0(2)	0.196(31)	0.009(33)	0.47(3)	−0.374(25)	$M1/E2$, $\frac{17}{2}^- \rightarrow \frac{15}{2}^-$
					0.46(3)	0.384(26)	$M1/E2$, $\frac{13}{2}^- \rightarrow \frac{15}{2}^-$
562.6	2560.1	13.7(2)	0.391(37)	−0.054(40)	0.23(12)	−0.044(53)	$E2$, $\frac{25}{2}^- \rightarrow \frac{21}{2}^-$ or $E2$, $\frac{21}{2}^- \rightarrow \frac{17}{2}^-$
614.9	1608.6	69.8(6)	0.360(21)	−0.065(22)	0.27(7)	0.026(35)	$E2$, $\frac{19}{2}^- \rightarrow \frac{15}{2}^-$
725.1	2333.7	44.2(5)	0.306(23)	−0.023(26)	0.37(6)	$0.052^{+0.043}_{-0.053}$	$E2$, $\frac{23}{2}^- \rightarrow \frac{19}{2}^-$
732.2	2340.8	3.4(2)	−0.236(115)	−0.097(109)	$0.20^{+0.45}_{-0.20}$	0.02(10)	$E1$, $\frac{21}{2}^+ \rightarrow \frac{19}{2}^-$ or $E1$, $\frac{17}{2}^+ \rightarrow \frac{19}{2}^-$
747.8	1657.6	9.5(3)	0.080(58)	0.131(61)	$0.43^{+0.27}_{-0.14}$	$-19.1^{+13.4}_{-\infty}$	$M1/E2$, $\frac{9}{2}^+ \rightarrow \frac{7}{2}^+$
760.5	909.8	9.9(2)	0.318(24)	−0.163(56)	0.30(8)	−1.35(20)	$M1/E2$, $\frac{7}{2}^+ \rightarrow \frac{7}{2}^+$
886.8	2495.4	6.9(2)	0.191(70)	−0.60(75)	0.39(25)	0.070(152)	$E2$, $\frac{23}{2}^- \rightarrow \frac{19}{2}^-$ or $\frac{15}{2}^- \rightarrow \frac{19}{2}^-$
					0.39(25)	0.84(51)	$M1/E2$, $\frac{19}{2}^- \rightarrow \frac{19}{2}^-$

[a] Uncertainties in the energy are ±0.3 keV.
[b] Seen in the preceding radiation; the intensity is too small to determine the angular distribution.
[c] The 407.7 keV transition in a composite peak; the intensity shown is an upper limit.

TABLE III. Transition energies, intensities, and experimental angular distribution results for ^{147}Eu.

E_γ[a] (keV)	Initial level (keV)	I_γ	A_{22}	A_{44}	σ/J	δ	Assignment
233	3230.1	b					
271.6	3795.2	8.9(2)	−0.205(47)	0.018(53)	$0.24^{+0.13}_{-0.24}$	−0.017(30)	$E1$, $\frac{31}{2}^- \rightarrow \frac{29}{2}^+$
290.3[c]	3191.2	1.0(1)	−0.307(108)	−0.103(120)	$0.19^{+0.30}_{-0.19}$	0.05(14)	$E1$, $\frac{29}{2}^+ \rightarrow \frac{27}{2}^-$
					$0.20^{+0.30}_{-0.20}$	0.09(12)	$E1$, $\frac{25}{2}^+ \rightarrow \frac{27}{2}^-$
293.5	3523.6	9.2(3)	−0.248(69)	0.011(65)	$0.20^{+0.10}_{-0.20}$	0.009(18)	$E1$, $\frac{29}{2}^+ \rightarrow \frac{27}{2}^-$
329.8	3230.1	5.4(1)	0.385(43)	−0.135(52)	$0.09^{+0.16}_{-0.09}$	−0.52(13)	$M1/E2$, $\frac{27}{2}^- \rightarrow \frac{27}{2}^-$
366.3	2293.2	57.7(5)	0.287(18)	−0.080(23)	0.30(3)	0.018(16)	$E2$, $\frac{23}{2}^- \rightarrow \frac{19}{2}^-$
369.5[c]	995.1	5.5(1)	0.361(37)	0.039(43)	0.39(6)	1.38(38)	$M1/E2$, $\frac{9}{2}^- \rightarrow \frac{11}{2}^-$
382.9	4178.1	6.6(1)	−0.338(37)	0.075(38)	$0.29^{+0.11}_{-0.16}$	0.061(50)	$E1$, $\frac{33}{2}^+ \rightarrow \frac{31}{2}^-$
421.1	2348.0	3.3(1)	−0.653(69)	−0.121(75)	$0.06^{+0.27}_{-0.06}$	$0.22^{+0.06}_{-0.11}$	$M1/E2$, $\frac{21}{2}^- \rightarrow \frac{19}{2}^-$
497.3[c]	2845.3	2.8(1)	−0.231(122)	0.115(137)	$0.39^{+0.24}_{-0.19}$	$7.12^{+\infty}_{-3.04}$	$M1/E2$, $\frac{23}{2}^- \rightarrow \frac{21}{2}^-$
					$0.32^{+0.19}_{-0.16}$	$-28.6^{+23.5}_{-\infty}$	$M1/E2$, $\frac{19}{2}^- \rightarrow \frac{21}{2}^-$
580.2	1926.9	93.8(11)	0.310(22)	−0.074(28)	$0.30^{+0.02}_{-0.03}$	0.009(10)	$E2$, $\frac{19}{2}^- \rightarrow \frac{15}{2}^-$
607.7	2900.9	37.2(5)	0.291(27)	−0.065(32)	0.30(5)	$0.009^{+0.025}_{-0.029}$	$E2$, $\frac{27}{2}^- \rightarrow \frac{23}{2}^-$
622.7	3523.6	9.6(2)	−0.268(37)	0.063(41)	$0.31^{+0.19}_{-0.31}$	0.026(65)	$E1$, $\frac{29}{2}^+ \rightarrow \frac{27}{2}^-$
648.9[c]	2996.9	6.0(1)	−0.485(43)	0.018(51)	$0.40^{+0.09}_{-0.07}$	$2.54^{+0.95}_{-0.60}$	$M1/E2$, $\frac{23}{2}^- \rightarrow \frac{21}{2}^-$
666.2	2012.9	2.1(2)	−0.391(226)	−0.306(206)			$M1/E2$, $\frac{13}{2}^- \rightarrow \frac{15}{2}^-$ or
							$M1/E2$, $\frac{17}{2}^- \rightarrow \frac{15}{2}^-$
704.4	2996.9	24.7(3)	0.225(23)	−0.033(28)	0.30(5)	0.384(40)	$M1/E2$, $\frac{23}{2}^- \rightarrow \frac{23}{2}^-$
721.1	1346.7	100(1)	0.272(21)	−0.055(26)	0.37(2)	0.009(9)	$E2$, $\frac{15}{2}^- \rightarrow \frac{11}{2}^-$
765[d]	995.1	<1					

[a] Uncertainties in the energy are ±0.3 keV.
[b] The 233 keV transition is composite with a strong 234 keV line from ^{148}Eu.
[c] Angular distribution data taken with 63 MeV ^{12}C ions.
[d] Seen in coincidence with the $\frac{7}{2}^+ \rightarrow$ g.s. transition; the intensity is too small to determine the angular distribution.

that unambiguous spin assignments were not possible. The angular distribution coefficients for the 429.5 keV transition are consistent within error with either a pure $E2$ or a mixed $M1/E2$ transition, for the same value of χ^2. A spin assignment of $\frac{19}{2}^-$ for the 932.2 keV level is unlikely since this assignment would suggest that this level is an yrast state and hence should be populated much more strongly. A $\Delta I = \pm 2$ assignment is consistent with the angular distribution for the 523.2 keV transition depopulating the 1455 keV level. The fact that the 932 and 1455 keV levels are so weakly populated suggests that they are probably members of the "unfavored" states, and the spin sequence for these levels could be $\frac{21}{2}^- \rightarrow \frac{17}{2}^-$ or $\frac{17}{2}^- \rightarrow \frac{13}{2}^-$.

B. ^{149}Eu

The ^{146}Nd(^{6}Li, $3n$) reaction at 32 MeV was used for the coincidence measurements and the ^{145}Nd(^{7}Li, $3n$) reaction at 32 MeV for the angular distribution experiments. Table II presents the information obtained from these measurements and Fig. 6 shows the level scheme deduced from it. Information on low-spin states in ^{149}Eu is available from the decay of ^{149}Gd (Ref. 11) and the nucleus has also been studied via the ^{151}Eu(p, t) reaction by Taketani *et al.*[4]

The main strength of the deexcitation proceeds through the decoupled band built on the 2.4 μsec $\frac{11}{2}^-$ state at 496 keV. Delayed coincidence measurements established the 725.1-614.9-498.1 keV cascade of stretched $E2$ transitions as preceding the $\frac{11}{2}^-$ state. The transition energies of the decoupled band are very similar to those of the adjacent even-even cores (see Fig. 5). The levels at 794, 1059, 1528, 1998, and 2560 keV may be the unfavored negative-parity states associated with the decoupled band. The 794 keV level is known from decay work and has been assigned as

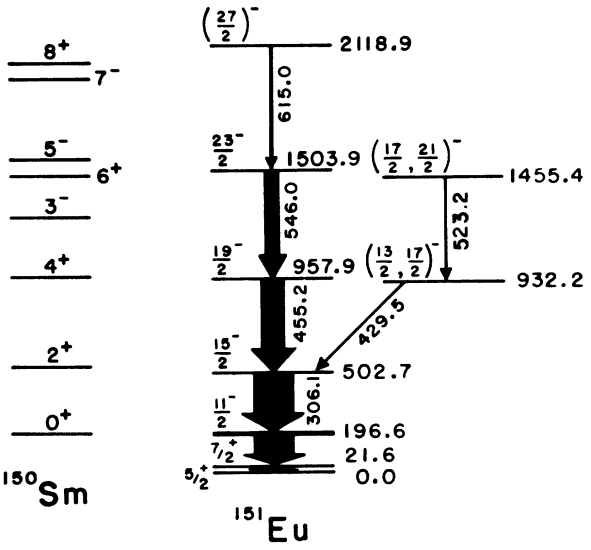

FIG. 4. ^{151}Eu level scheme. Widths of arrows are proportional to the photon intensities. The 21.6 keV, $\frac{7}{2}^+ \rightarrow \frac{5}{2}^+$, transition was not observed in this study for technical reasons.

$\frac{9}{2}^-$ but the 265 keV transition that populates this level is an unresolved triplet and so a spin assignment could not be made for the 1059 keV level. No other transitions were observed populating or depopulating this level within the detection limit of the coincidence experiment (any transition having an intensity greater than 0.01 times that of the $\frac{15}{2}^-$ to $\frac{11}{2}^-$ transition should have been observed). The 533.8 and 388.6 keV transitions appear to be $M1/E2$ transitions while the 470.0 and 562.6 keV transitions have a quadrupole-octupole mixing parameter $\delta_{23} \approx 0$ and a $\Delta I = \pm 2$ angular distribution, suggesting an $E2$ assignment. Therefore two spin sequences are possible for the levels at 1528, 1998, and 2560 keV; either $\frac{13}{2}^-$, $\frac{17}{2}^-$, and $\frac{21}{2}^-$, respectively, or $\frac{17}{2}^-$, $\frac{21}{2}^-$, and $\frac{25}{2}^-$.

The levels at 2341, 2574, and 3042 keV are connected to the decoupled $\frac{11}{2}^-$ band by transitions with, at most, small admixtures of quadrupole radiation, thus suggesting $E1$ assignments for these transitions and positive parity for these levels. Since no transitions to lower-spin states are observed from these levels a weak argument can be made for a $\Delta I = -1$ character for the 174.9, 240.7, 292.7, and 732.2 keV transitions. A smoothly increasing function of energy vs spin would be expected for the yrast levels and since the levels at 2574, 2749, and 3042 appear to belong to the yrast cascade, a $\Delta I = -1$ assignment for the transitions depopulating these levels would not be unreasonable.

Three other low-spin states were observed. The level at 666 keV has been assigned as $\frac{5}{2}^+$, $\frac{7}{2}^+$, $(\frac{9}{2}^+)$ by Eppley, McHarris, and Kelly[11] in studies of the electron-capture decay of ^{149}Gd; our in-beam angular distribution data favor the as-

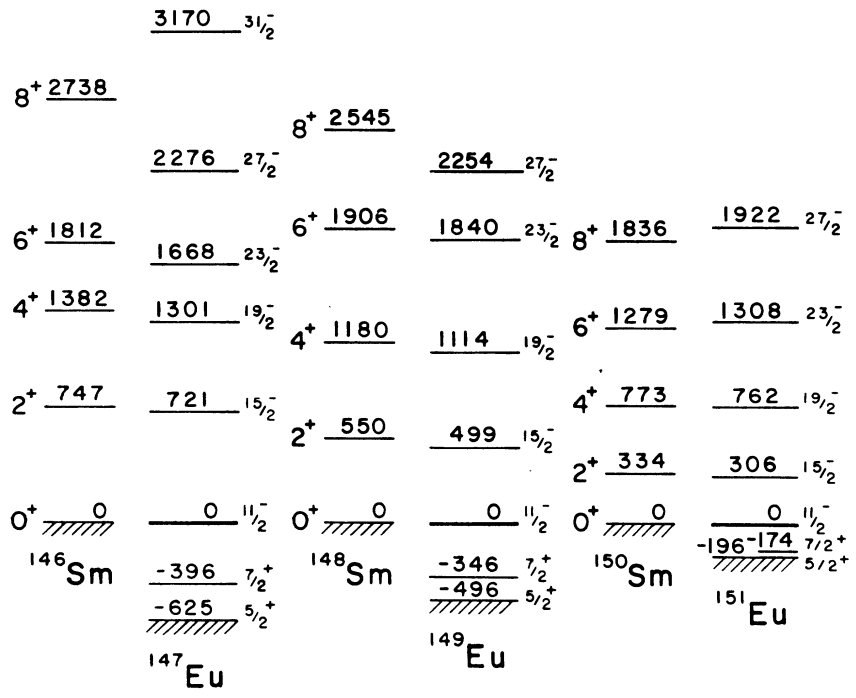

FIG. 5. Comparison between the "decoupled" bands of the odd-A Eu nuclei and the adjacent even-A Sm cores.

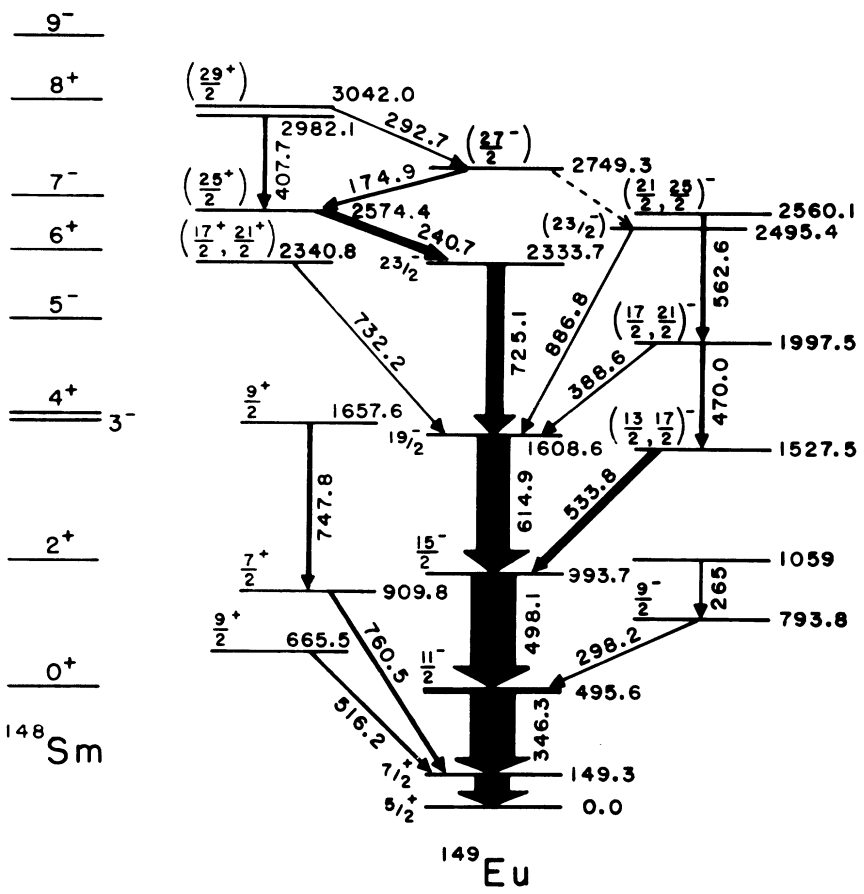

FIG. 6. ^{149}Eu level scheme. The 407.7 keV transition is part of a composite peak and the intensity shown is an upper limit.

signment of $\frac{9}{2}^+$ for this level. The level observed at 910 keV is probably the same level as that reported at 911 keV in the (p, t) reaction studies of Taketani *et al.*[4] The (p, t) data rule out $\Delta L = 0$ transfer and the assignment of $\frac{5}{2}^+$ for this level, while the angular distribution data from our work favor an assignment of $\frac{7}{2}^+$. The level at 910 keV is populated by the 747.8 keV transition from the level at 1658 keV and the angular distribution data are consistent with an assignment of $\frac{9}{2}^+ - \frac{7}{2}^+$ with $\delta_{12} = -19.1$ for the 747.8 keV transition.

C. ^{147}Eu

The coincidence measurements were taken using the ^{143}Nd(^{7}Li, $3n$) reaction and the angular distribution measurements were obtained with the ^{139}La(^{12}C, $4n$) reaction at 60 and 63 MeV. The latter reaction was chosen due to the larger yield for higher-spin states. Table III summarizes the information obtained from these measurements and Fig. 7 shows the decay scheme based on this information. Knowledge of low-spin states in ^{147}Eu is limited to results from the studies[6] of the decay of ^{147}Gd.

Again the main strength of the decay proceeds through the decoupled band. The energies of the first three transitions in the decoupled band are very similar to those of the ^{146}Sm core (see Fig. 5). Possible members of the unfavored states are observed at 995, 2013, 2348, 2845, 2997, and 3230 keV. The 995 keV level is known from the decay of ^{147}Gd and has previously been assigned a spin and parity of $\frac{9}{2}^-$, a value which is confirmed by this work. A spin assignment of $\frac{17}{2}^-$ or $\frac{13}{2}^-$ has been made for the 2013 keV state since the 666.2 keV transition to the 1347 keV states has an angular distribution consistent with a $\Delta I = \pm 1$ assignment and a large δ_{12}. The level at 2348 keV is populated by the 648.9 keV transition and depopulated by the 421.1 keV transition. The angular distributions for these transitions indicate appreciable values of δ_{12} and therefore $M1/E2$ mixtures are most likely. The 55 keV transition between the 2348 and the 2293 keV states was not directly observed in the coincidence experiments due to

the low efficiency of the detector at this energy, but its existence is indicated by the fact that the 648.9 keV transition is observed to be in coincidence with the 366.3 keV transition. Angular distribution data for the 293.5 and 329.8 keV transitions establish the spin of the 3230 keV level as $\frac{27}{2}^-$ (if the 3524 keV level is $\frac{29}{2}$). This requires the 233 keV transition to be $E2$ since the 704.4 keV transition which depopulates the 2997 keV level appears to be a $\Delta I = 0$ or ± 2 transition. The angular distribution data for the 233 keV transition are not inconsistent with this assignment although the conclusions based upon the data are uncertain since this transition is composite with a 234 keV line in ^{148}Eu. The spin assignments for the 2997 and 3230 keV levels are therefore limited to $\frac{23}{2}^-$ and $\frac{27}{2}^-$, respectively.

The levels at 3524 and 4178 keV are linked to the decoupled band by transitions assigned as $E1$, on the basis of angular distributions consistent with $\Delta I = \pm 1$ and $\delta_{12} \approx 0$. These proposed high-spin positive-parity states are similar to those observed in ^{149}Eu and in both nuclei it appears that the yrast cascade proceeds back and forth between these levels and high-lying negative-parity levels. As was the case for ^{149}Eu, an argument for $\Delta I = -1$ assignments for the 382.9, 271.6, and 662.7 keV transitions can be made on the basis of

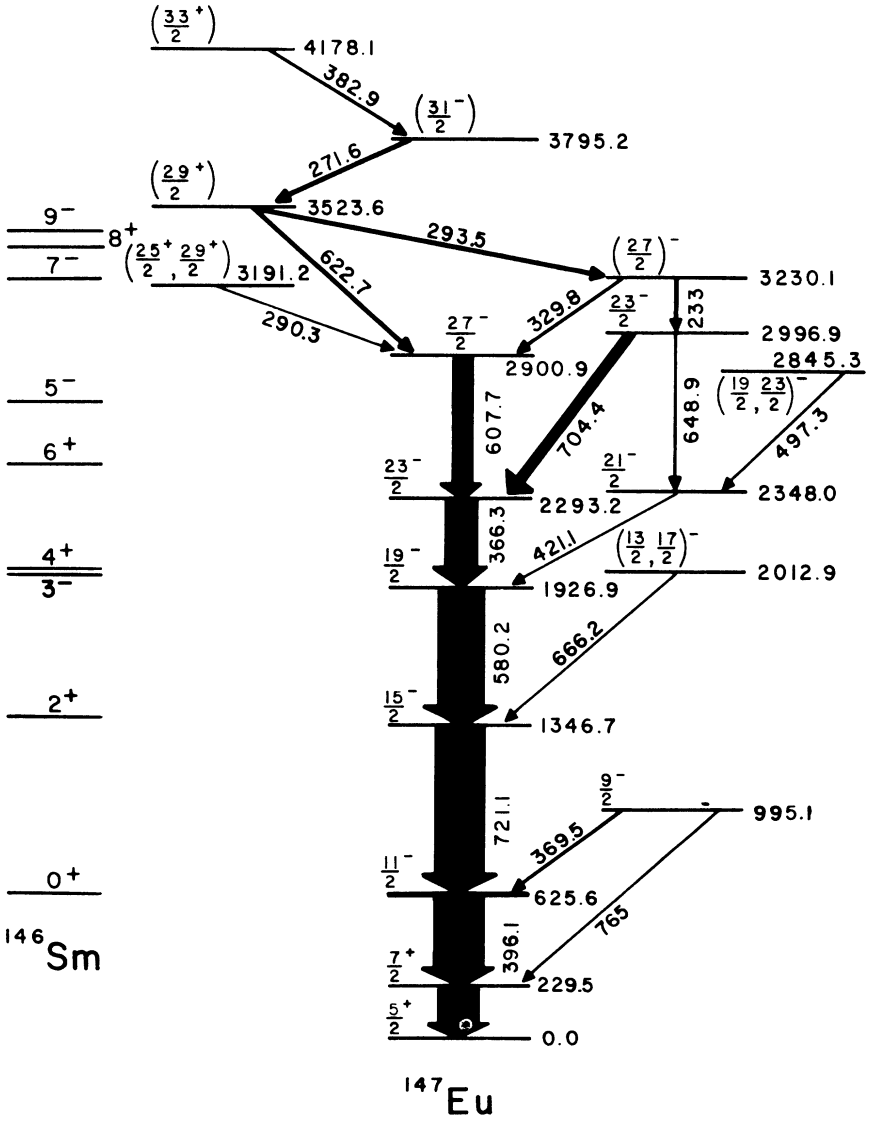

FIG. 7. ^{147}Eu level scheme. The 234 keV transition is part of a composite peak with a transition in ^{148}Eu and the intensity shown is a lower limit.

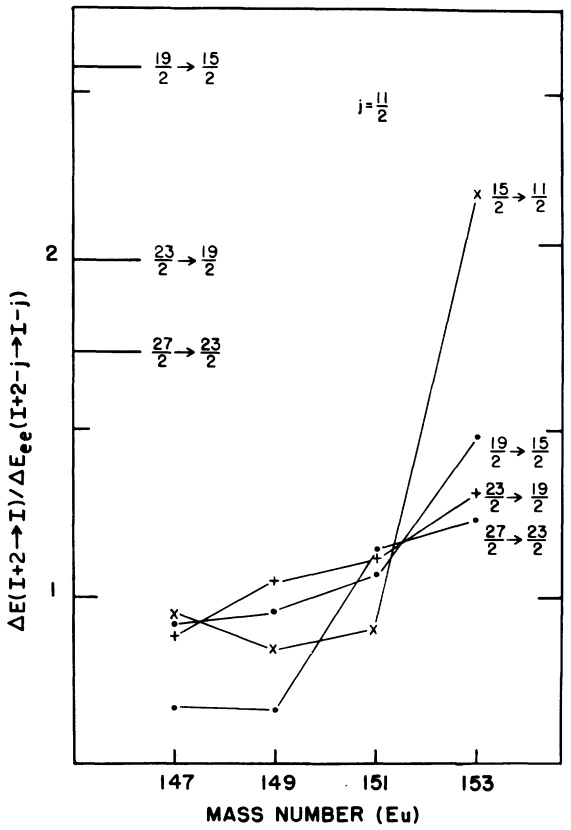

FIG. 8. The ratio of $\Delta E(I+2 \rightarrow I)$ in the odd-A Eu nuclei and the corresponding energies in the adjacent e-e core nuclei plotted versus mass number. Rotational-band and decoupled-band limits are shown along with the data for the first four transitions in the $h_{11/2}$ band. The data for ^{153}Eu are from Ref. 13.

a smoothly increasing function of energy versus spin for members of the yrast cascade. The 3191 level is depopulated only by the 290.3 keV transition which has a distribution consistent with a $\Delta I = \pm 1$ assignment and $\delta_{12} = 0$, and an $E1$ assignment for the 290.3 keV transition is favored.

IV. DISCUSSION

The europium nuclei studied in this work lie in the so-called "transitional" region between the closed shell at $N = 82$ and on the onset of the deformed region at $N = 90$. The position of the members of the quasi-ground-state band having $I \leq 4$ and the lower lying negative-parity states in the core nuclei exhibit a relatively smooth transition from the "vibrational" ^{146,148}Sm and ^{148,150}Gd to the "rotational" ^{150}Sm and ^{152}Gd (Ref. 12). The average of the energies of the first 2^+ states of the adjacent even-even core nuclei is 747 keV for the case of ^{147}Eu, 596 keV for ^{149}Eu, and 339 keV for ^{151}Eu. It is of interest to note that the $6^+ \rightarrow 4^+$ energy spacing is less than the $4^+ \rightarrow 2^+$ energy spacing in ^{146}Sm. As was noted in Sec. III the energy spacings in the "decoupled" bands of ^{147,149,151}Eu bear a close resemblance to the ground-state bands of these core nuclei. Figure 8 is a plot similar to that of Stephens[1] showing the ratio of $\Delta E(I+2 \rightarrow I)$ for the odd mass nucleus and the average of the corresponding transition energies in the adjacent even-even nuclei $\Delta E(I+2-j \rightarrow I-j)$ plotted vs mass number of the odd-A Eu isotopes. The data for ^{153}Eu are from Ref. 13. The decoupled band limit (where the odd particle is completely decoupled from the core) is 1.0, and the rotational band limits are shown. The energy ratios show a slight increase with mass number and this might be attributed to both an increase in the deformation parameter β and an increase in the energy of the Fermi level with mass number. However, the energy ratios are all reasonably close to the decoupled band limit suggesting that ^{147}Eu, ^{149}Eu, and ^{151}Eu all have essentially pure decoupled bands even for the lower-spin members. With the exception of the decoupled band and its associated unfavored states there seem to be no other levels observed using the reactions employed in the present work which correspond to the coupling of the odd particle to positive-parity states of the core (e.g., quasi-β or -γ band states).

The decoupled band structure does not seem to extend above spin $\frac{23}{2}$ for ^{147}Eu and ^{149}Eu. Although $\frac{27}{2}^-$ levels are seen, no $E2$ transitions are observed to the $\frac{23}{2}^-$ level in ^{149}Eu and the level spacing of the $\frac{27}{2}^-$ and $\frac{23}{2}^-$ levels does not resemble that of the corresponding level spacing of the core nucleus for either ^{147}Eu or ^{149}Eu. The $\frac{27}{2}^-$ level in the decoupled case would correspond to the odd particle coupled to an $R = 8$ angular momentum state of the core. However, the 8^+ yrast states of the adjacent e-e core nuclei for ^{147}Eu and ^{149}Eu are thought to be predominantly two quasiparticle in nature,[14] i.e., $\nu(f_{7/2}{}^1 h_{9/2}{}^1)$. The coupling of the odd particle to a two quasiparticle excitation of the core has also been observed in the Hg and Pt isotopes[15-17] where the odd particle is an $i_{13/2}$ neutron. For the Hg cases, the 10^+ and to a lesser extent the 8^+ levels of the ground-state band of the core nuclei are composed predominantly of a two proton hole configuration $(\pi h_{11/2}{}^{-2})$. The energy difference between the 8^+ and 10^+ levels in ^{192}Hg and ^{194}Hg is about 60 keV while the corresponding transition energy in the decoupled band is approximately 180 keV for ^{191,193,195}Hg. Thus the three quasiparticle nature of the $\frac{27}{2}^-$ levels in ^{147}Eu and ^{149}Eu may explain why the decoupled band structure does not extend above spin $\frac{23}{2}$.

The possible $\frac{25}{2}^+$ levels at 2574 keV in ^{149}Eu and at 3191 keV in ^{147}Eu are very close to the excitation

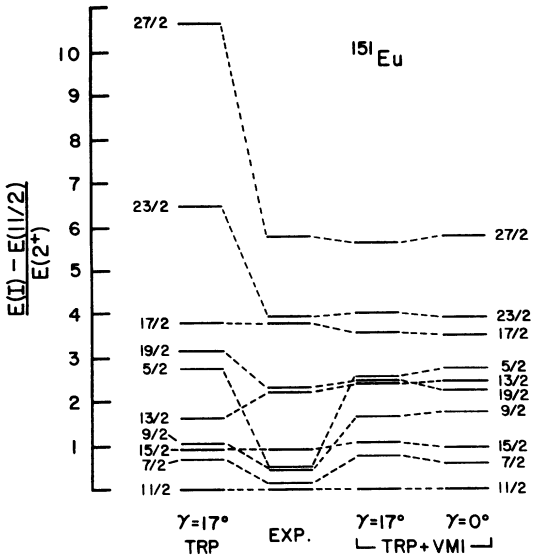

FIG. 9. Comparison between theoretical and experimental energies of the negative-parity states associated with the $h_{11/2}$ system. Columns 3 and 4 show the results of the TRP calculations including a variable moment of inertia (VMI). Column 3 is the asymmetric case with "best fit" parameters of $\gamma = 17.0°$, $\beta = 0.165$, and $\lambda_f = 1.30$ (see Ref. 2). Column 4 is the symmetric case ($\gamma = 0°$) with best fit parameters of $\beta = 0.155$ and $\lambda_f = 1.55$. Column 1 presents the results of the TRP model with no VMI.

energies of the 7^- levels in the core nuclei and these levels may be due to an $h_{11/2}$ particle coupled to the 7^- state of the core. In addition the possible $\frac{29}{2}^+$ levels at 3042 and 3524 keV in ^{149}Eu and ^{147}Eu, respectively, may be due to an $h_{11/2}$ particle coupled to the 9^- core state. High-spin positive-parity levels have also been observed in the odd neutron $N = 77$ isotones from Xe to Nd. It has been proposed that the $\frac{19}{2}^+$ levels in ^{131}Xe, ^{133}Ba, ^{135}Ce, and ^{137}Nd are due to the $h_{11/2}$ nucleon coupled to the 5^- level in the core nuclei. It is not clear whether these 5^- levels arise from proton or neutron configurations.[18] Similarly, high-spin negative-parity bands have been observed in ^{191,193}Hg (Ref. 14) and ^{191,193}Pt (Ref. 16). The energy spacing between the members of these bands resembles very closely those in the $I^\pi = 5^-, 7^-, 9^-, \ldots$, band in the adjacent even Hg isotopes. These bands have been attributed to an $i_{13/2}$ particle coupled to the negative-parity band of the core nucleus.

The aligned states are usually strongly populated in (HI, xn) reactions and they have been described by many models. However, the unfavored states, usually weakly populated, provide a much better test of the model employed. The triaxial rotor-plus-particle model of Meyer-ter-Vehn[2] has had some success in qualitatively explaining the odd-parity bands based upon $\frac{9}{2}^-$ and $\frac{11}{2}^-$ states in the $A = 135$ and $A = 190$ mass regions. We have employed this model in an attempt to explain the negative-parity structure of ^{149}Eu and ^{151}Eu even though the even-parity level structure for the core nuclei is not suggestive of triaxiality. Calculations by Andersson *et al.*[19] have shown a tendency for changes in the shape of the core nuclei as the angular momentum increases and it is possible that the odd-A nuclei may become triaxial due to the presence of the odd particle.

The results of the triaxial rotor-plus-particle (TRP) model are shown in column 1 in Figs. 9 and 10. The discrepancy between theory and experiment increases with increasing spin. This effect has been noted before in other TRP calculations and as Toki and Faessler[3] have shown, can be compensated for by including a variable moment of inertia (VMI) treatment in the calculations. We have incorporated a VMI treatment in our TRP calculations since the core nuclei for ^{149}Eu and ^{151}Eu can be described very well by the VMI model. Our approach is the same as that of Toki and Faessler with two minor variations. First, the "restoring force constant" C and the "ground-state moment of inertia" ϑ_0 were determined from the decoupled band rather than the adjacent even-even core since the presence of the odd particle

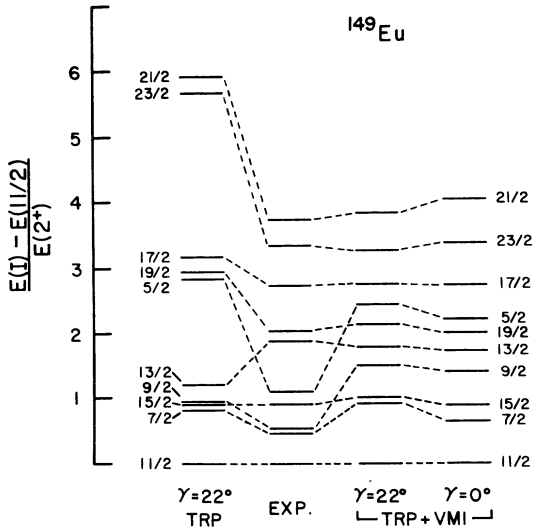

FIG. 10. Comparison between theoretical and experimental negative-parity levels built on the $\frac{11}{2}^-$ intrinsic state for ^{149}Eu. "Best fit" parameters for the asymmetric case are $\gamma = 22.0°$, $\beta = 0.120$, and $\lambda_f = 1.15$. "Best fit" parameters for the symmetric case are $\beta = 0.115$ and $\lambda_f = 1.65$.

may change the core deformation. The difference in the two approaches does not have a major effect on the results. Secondly, the rotational energy for the even core in the VMI treatment is

$$E_R = \frac{1}{2\mathcal{I}} R(R+1) + \tfrac{1}{2} C(\mathcal{I} - \mathcal{I}_0)^2 \quad (1)$$

or alternately

$$E_R = \frac{1}{2\mathcal{I}_{\text{eff}}} R(R+1) , \quad (2)$$

where

$$\mathcal{I}_{\text{eff}} = \mathcal{I}\left(1 + \frac{\mathcal{I} C(\mathcal{I} - \mathcal{I}_0)^2}{R(R+1)}\right)^{-1} . \quad (3)$$

The use of $\mathcal{I}$ in the TRP model tends to make the core too "soft," that is, it tends to predict too low an energy for the high-spin states, whereas by using $\mathcal{I}_{\text{eff}}$ as the moment of inertia a much better fit to the experimental decoupled band can be achieved. Columns 3 and 4 in Figs. 9 and 10 present the best fits to the experimental data for the asymmetric case ($\gamma \neq 0°$) and the symmetric case ($\gamma = 0°$). The overall agreement between theory and experiment is very good (with the exception of the $\frac{5}{2}$ and $\frac{9}{2}$ states) and may indicate a slight preference for triaxiality. The fits were obtained by varying β, γ, and the Fermi level λ_f. Initial values for the parameters β and γ were obtained from the adjacent e-e cores according to the Meyer-ter-Vehn prescription. The minimization of χ^2 was performed only for the states with $I \geq \frac{11}{2}$ due to the poor agreement between theory and experiment for the $\frac{5}{2}$ and $\frac{9}{2}$ states. The "best fit" values of β and γ did not differ much from the initial values for the asymmetric case; for example, core values of γ for ^{151}Eu and ^{149}Eu were 17° and 20°, respectively, while the best fit values were 17° and 22°, respectively. However, in both the symmetric and asymmetric cases the deformation β was about 15–20% smaller than the core values. For ^{151}Eu the value of χ^2 is essentially the same for the symmetric and asymmetric cases, yet the correct level ordering for the $\frac{13}{2}$ and $\frac{19}{2}$ levels is preserved only for the asymmetric case. For ^{149}Eu the value of χ^2 for the asymmetric fit is about one-half that for the symmetric fit. This is due to the better fit of the unfavored states in the asymmetric case.

The TRP model was not used to describe the negative-parity levels of ^{147}Eu since the core nuclei do not exhibit rotational characteristics. On the other hand, the close resemblance of the energy spacings of ^{147}Eu and those of the ^{146}Sm and ^{148}Gd core nuclei gives evidence for particle core coupling in ^{147}Eu. The positive-parity levels of ^{146}Sm have been described by Heyde and Brussaard[20] in terms of the coupling of two $f_{7/2}$ valence neutrons to one, two, and three quadrupole phonon states of the $N = 82$ core. A quintet of negative-parity states has been calculated by Vogel and Kocbach[21] for the simultaneous excitation of one quadrupole and one octupole phonon. Above 2.3 MeV this vibrational description breaks down and states above 3 MeV can be explained by excitations of two neutrons outside the $N = 82$ closed shell. Similar results have also been obtained for the $N = 84$ isotone ^{144}Nd (Ref. 22).

V. CONCLUSIONS

Bands with $\Delta I = 2$ built on the $\frac{11}{2}^-$ isomeric state have been observed in ^{147,149,151}Eu along with possible unfavored states associated with the $h_{11/2}$ system. In addition, high-spin positive-parity states have been observed in ^{147,149}Eu which may be due to the coupling of the odd particle to octupole states of the core. The negative-parity level structure of ^{149,151}Eu has been described by the triaxial rotor-plus-particle model incorporating a variable moment of inertia. The calculations are slightly more consistent with a triaxial description of the core, but the choice between asymmetric and symmetric descriptions of the core is not definitive. Branching ratio calculations were not performed due to the lack of experimental data since the (^{6,7}Li, $xn\gamma$) reactions primarily populated yrast states and the unfavored states were very weakly populated. The $N = 88$ isotones ^{153}Tb and ^{155}Ho have been investigated by Devous[23] via the ($\alpha, 4n\gamma$) and (^{10}B, $5n\gamma$) reactions, respectively, and the decoupled band structure of both ^{153}Tb and ^{155}Ho is similar to that of ^{151}Eu. The level structure of both these nuclei can be described with the assumption that they are weakly deformed. The study of other $N = 84, 86$ isotones would be helpful in understanding the systematics of this region. We are presently investigating the lighter mass ($A < 147$) Eu isotopes.

ACKNOWLEDGMENTS

The authors would like to thank David Rakel, Stephen Rozak, and Dr. G. Neal for their assistance in data collection and Dr. P. R. Chagnon, Dr. Roger West, Dr. E. Berners, and James Kaiser for their technical assistance. They would also like to thank Dr. T. L. Khoo and Dr. F. W. Bernthal for supplying the computer code for the triaxial rotor calculations.

*Supported in part by the National Science Foundation.

[1]F. S. Stephens, Rev. Mod. Phys. 47, 43 (1975).
[2]J. Meyer-ter-Vehn, Nucl. Phys. A249, 111, 141 (1975).
[3]H. Toki and A. Faessler, Nucl. Phys. A253, 231 (1975).
[4]H. Taketani, H. L. Sharma, and N. M. Hintz, Phys. Rev. C 12, 108 (1975).
[5]D. G. Burke, G. Løvhøiden, and J. C. Waddington, Phys. Lett. 43B, 470 (1973).
[6]E. P. Grigor'ev, A. V. Zolotavin, V. O. Sergeev, and N. A. Tikhonov, Izv. Akad. Nauk SSSR, Ser. Fiz. 36, 76 (1972) [Bull. Acad. Sci. USSR, Phys. Ser. 36, 75 (1972)].
[7]G. E. Holland, Nucl. Data Sheets 19, 337 (1976).
[8]B. Harmatz, Nucl. Data Sheets 19, 33 (1976).
[9]E. M. Bernstein, G. R. Boss, G. Hardie, and R. E. Shamu, Phys. Lett. 33B, 465 (1970).
[10]O. Straume, G. Løvhøiden, and D. G. Burke, Nucl. Phys. A266, 390 (1976).
[11]R. E. Eppley, Wm. C. McHarris, and W. H. Kelly, Phys. Rev. C 2, 1077 (1970).
[12]J. Kownacki, Z. Sujkowski, H. Ryde, and I. Adam, in *Proceedings of the International Conference on Nuclear Structure and Spectroscopy, Amsterdam, 1974,* edited by H. P. Blok and A. E. L. Dieperink (Scholar's Press, Amsterdam, 1974), p. 103.
[13]G. D. Dracoulis, J. R. Leigh, M. G. Slocombe, and J. O. Newton, J. Phys. G 1, 853 (1975).
[14]R. Arlt *et al.*, Izv. Akad. Nauk SSSR Ser. Fiz. 36, 2074 (1972).
[15]R. M. Lieder *et al.*, Nucl. Phys. A248, 317 (1975).
[16]M. Piiparinen *et al.*, Phys. Rev. Lett. 34, 1110 (1975).
[17]S. K. Saha *et al.*, Phys. Rev. C 15, 94 (1977).
[18]J. Gizon, A. Gizon, and D. J. Horen, Nucl. Phys. A252, 509 (1975).
[19]G. Andersson *et al.*, Nucl. Phys. A268, 205 (1976).
[20]K. Heyde and P. J. Brussaard, Nucl. Phys. A104, 81 (1967).
[21]P. Vogel and L. Kocbach, Nucl. Phys. A176, 33 (1971).
[22]L.-E. DeGeer *et al.*, Nucl. Phys. A259, 399 (1976).
[23]M. D. Devous, Ph.D. thesis, University of Texas A & M (unpublished).